L-carnitine attenuates TGF-β1-induced EMT in retinal pigment epithelial cells via a PPARγ-dependent mechanism

MIN LI, HUI LI, SHUAI YANG, XIN LIAO, CHUN ZHAO and FANG WANG

Department of Ophthalmology, Shanghai Tenth People's Hospital, Shanghai 200072, P.R. China

Received September 8, 2020; Accepted March 4, 2021

DOI: 10.3892/ijmm.2021.4943

Abstract. The epithelial-mesenchymal transition (EMT) of retinal pigment epithelial (RPE) cells is an important underlying mechanism of proliferative vitreoretinopathy (PVR). We previously found that L-carnitine (β-hydroxy-γ-N-trimethylammonium-butyrate, LC) was significantly lower during the transforming growth factor-β1 (TGF-β1)-induced EMT process in ARPE-19 cells. The present study assessed the role of LC in the EMT of RPE cells. The migration of RPE cells was detected using a Transwell migration assay. Then, EMT-related biomarkers were measured via western blotting, immunofluorescence and reverse transcription-quantitative PCR. It was observed that LC attenuated the TGF-β1-induced downregulation of the epithelial markers E-Cadherin and zonula occludens-1, as well as the expression of mesenchymal markers fibronectin and α-smooth muscle actin. Meanwhile, LC blocked Erk1/2 and JNK pathways in the EMT of RPE cells. Moreover, treatment with a peroxisome proliferator-activated receptor γ (PPARγ) inhibitor prevented the effect of LC on EMT. Taken together, these data suggested that LC attenuated EMT induced by TGF-β1 via inhibition of the Erk1/2 and JNK pathways and upregulation of PPARγ expression.

Introduction

Proliferative vitreoretinopathy (PVR) is a disease that develops as a complication following retinal detachment surgery (1). It is characterized by the presence of epiretinal membranes (ERM) that exert traction by re-detachment of the retina (2). The epithelial-mesenchymal transition (EMT) of retinal pigment epithelial (RPE) cells has been recognized as an important mechanism that contributes to ERM formation (3,4). EMT can be triggered by a number of molecules, including fibroblast growth factor (5) and epidermal growth factor (6). However, transforming growth factor-β1 (TGF-β1) is still considered to be the primary trigger of EMT (7-9). Our previous study also provided evidence that TGF-β1 plays a vital role in the EMT of the human RPE cell line, ARPE-19 (10,11).

Peroxisome proliferator-activated receptor γ (PPARγ) is a member of the peroxisome proliferator-activated receptor (PPAR) family. Previous studies have demonstrated that PPARs play important roles in the regulation of proinflammatory cytokine expression (12) and tissue fibrosis (13,14). Furthermore, PPARγ inhibits the induction of EMT via TGF-β1 in alveolar epithelial cells in humans (15). In RPE cells, PPARγ regulates inflammation through monocyte chemoattractant protein-1 (16) and major histocompatibility complex class II molecule expression (17). Nevertheless, to the best of our knowledge, there has been no investigation of the role of PPARγ in the EMT of RPE cells.

L-carnitine (β-hydroxy-γ-N-trimethylammonium-butyrate, LC) is essential for lipid energy metabolism via β-oxidation of long-chain fatty acids (18). Using metabolomics approaches, we previously found that LC was significantly reduced in the vitreous of patients with PVR (19). Baci *et al* (20) reported that LC had anti-angiogenic and anti-inflammatory effects via nuclear factor-κB (NF-κB), and inhibition of vascular endothelial growth factor (VEGF) and VEGF receptor 2. Of note, LC has also been illustrated to attenuate kidney fibrosis in hypertensive rats by upregulating PPARγ (21). However, whether LC has an effect on the EMT of RPE cells has not yet been elucidated, and if there is an effect the underlying mechanism is not known. In the present study, it was found that LC attenuated EMT induced by TGF-β1 via inhibition of the Erk1/2 and JNK pathways and upregulation of PPAR-γ expression.

Materials and methods

Cell culture. Human RPE cells were obtained from the healthy eyes of donors according to a previously published report (22). Primary RPE cells were cultured and 2-5 generation cells were used in this study. ARPE-19 cells were purchased from NewGainBio. Primary RPE cells and ARPE-19 cells were routinely cultured in DMEM/F12 (Gibco; Thermo Fisher Scientific, Inc.) with 100 U/ml penicillin and 100 μg/ml streptomycin (Beijing Solarbio Science & Technology Co., Ltd.) at 37˚C in a cell incubator containing 5% CO_2. The medium was changed every 2 days. ARPE-19 cells and human RPE cells were

Correspondence to: Professor Fang Wang, Department of Ophthalmology, Shanghai Tenth People's Hospital, 301 Middle Yanchang Road, Shanghai 200072, P.R. China
E-mail: fwang7527@163.com

Key words: proliferative vitreoretinopathy, epithelial-mesenchymal transition, retinal pigment epithelial cell, L-carnitine

starved in serum-free medium for 16 h. Cells were then incubated with 10 ng/ml TGF-β1 with or without LC (Sigma-Aldrich; Merck KGaA) at the indicated concentrations (0.1, 1 and 10 μM) at 37˚C for 24 or 48 h. This study was approved by the Ethics Committee of Shanghai Tenth People's Hospital (approval no. SHSY-IEC-KY-4.0/17-79/01; Shanghai, China) and was in compliance with the Declaration of Helsinki. Donors' eyes were obtained from the Eye Bank of Shanghai Tenth People's Hospital.

Transwell migration assay. A total of $1x10^6$ RPE cells were plated into the upper chambers of Transwell plates (8-mm pore size; Costar, Inc.) in 100 ml DMEM with 0.5% FBS (Invitrogen; Thermo Fisher Scientific, Inc.). Medium with 10% FBS were added into the lower chambers. After 24 or 48 h, the upper chambers of the Transwell plates were fixed with 4% paraformaldehyde for 30 min at room temperature and stained with 0.1% crystal violet for 20 min at room temperature. Five fields of migrated cell numbers were counted in each chamber with a fluorescence microscope (Olympus Corporation).

Immunofluorescence analysis. After TGF-β1 and LC treatment, RPE cells were fixed with 4% paraformaldehyde for 10 min at room temperature and blocked with 10% bovine serum albumin (MP Biomedicals, LLC) for 1 h at room temperature. Then, RPE cells were stained with the primary antibodies at 4˚C overnight, followed by incubation with the FITC-conjugated secondary antibody (1:500; cat. no. ab8503; Abcam) at room temperature for 1 h. The nuclei were stained with DAPI for 5 min at room temperature, and subsequently cell images were captured using a fluorescence microscope at x400 magnification (Olympus Corporation). The following primary antibodies were used: Rabbit anti-cellular retinaldehyde-binding protein (CRALBP; 1:500; cat. no. ab243664; Abcam), anti-retinoid isomerohydrolase (RPE-65; 1:250; cat. no. ab231782; Abcam), mouse anti-α-smooth muscle actin (α-SMA; 1:50; cat. no. ab7817; Abcam), anti-zonula occludens-1 (ZO-1; 1:1,000; cat. no. ab276131; Abcam) and anti-E-Cadherin (1:500; cat. no. AF748; R&D Systems, Inc.).

Reverse transcription-quantitative (RT-q)PCR. Total RNA was extracted using TRIzol® reagent (Invitrogen; Thermo Fisher Scientific, Inc.). cDNA was synthesized using a reverse transcription kit (Takara Bio, Inc.), according to the manufacturer's protocols. RT-qPCR was performed using a 7500 Fast Real-time PCR System (Applied Biosystems; Thermo Fisher Scientific, Inc.) with SYBR Green (Beijing Solarbio Science & Technology Co., Ltd.) Specific primers were purchased from Gentec (Shanghai) Corporation, with GAPDH used as an internal control. The thermocycling conditions were as follows: 94˚C for 30 sec, 40 cycles of 94˚C for 5 sec and 60˚C for 30 sec. The $2^{-\Delta\Delta Cq}$ method (23) was used to measure the relative expression of each gene. All reactions were repeated three times. The primers are presented in Table I.

Western blotting. RPE cells were lysed with RIPA buffer (Beyotime Institute of Biotechnology) on ice for 30 min and then centrifuged at 10,000 x g for 10 min at 4˚C. The total protein of the supernatant was quantified using a bicinchoninic acid protein assay (Pierce; Thermo Fisher Scientific, Inc.). Then, 350 μg protein/lane was separated via SDS-PAGE on 6-12% gels, and subsequently separated proteins were transferred to PVDF membranes (EMD Millipore) and blocked in 5% non-fat milk for 1 h at room temperature. Membranes were then incubated overnight at 4˚C with the following primary antibodies: Anti-α-SMA (1:200; cat. no. ab7817; Abcam), anti-ZO-1 (1:1,000; cat. no. ab276131; Abcam), anti-E-Cadherin (1:500; cat. no. AF748; R&D Systems, Inc.), anti-fibronectin (FN; 1:500; cat. no. ab2413; Abcam), anti-JNK (1:1,000; cat. no. ab179461; Abcam), anti-phosphorylated (p)-JNK (1:1,000; cat. no. ab124956; Abcam), anti-Erk1/2 (1:10,000; cat. no. ab184699; Abcam), anti-p-Erk1/2 (1:400; cat. no. ab218017; Abcam), anti-p38 (1:1,000; cat. no. ab170099; Abcam), anti-p-p38 (1:1,000; cat. no. A1984; BioVision, Inc.), p-p105 (1:1,000; cat. no. bs-0465R; BIOSS), anti-p-p65 (1:1,000; cat. no. AF5881; Beyotime Institute of Biotechnology), anti-p-IκBα (1:1,000; cat. no. 4814; Cell Signaling Technology, Inc.), anti-PPARγ (1:10,000; cat. no. ab178860; Abcam), anti-N-cadherin (1:1,000; cat. no. 13116; Cell Signaling Technology, Inc.), anti-vimentin (1:1,000; cat. no. 5741; Cell Signaling Technology, Inc), anti-Snail (1:1,000; cat. no. 3879; Cell Signaling Technology, Inc.) and anti-GAPDH (1:1,000; cat. no. 5174; Cell Signaling Technology, Inc). The membrane was then incubated with the secondary antibodies (1:10,000; cat. nos. w4011 and S3721; Promega Corporation) at room temperature for 1 h. SB203580 (25 mM), SP600125 (100 mM), BAY11-7082 (100 mM) and GW9662 (50 mM) were purchased from Abcam. U0126 (100 mM) was purchased from Beyotime Institute of Biotechnology. The blots were scanned using Image Quant LAS 4000 (Cytiva) and analyzed with ImageJ version 2 software (National Institutes of Health).

Statistics. At least three independent experiments were performed. Data are presented as the mean ± standard deviation,

Table I. Primers used for reverse transcription-quantitative PCR.

Genes	Primer sequences (5'→3')
ZO-1	F: TGAGGCAGCTCACATAATGC
	R: GGTCTCTGCTGGCTTGTTTC
E-cadherin	F: TGCCCAGAAAATGAAAAAGG
	R: GTGTATGTGGCAATGCGTTC
α-SMA	F: AGCAGGCCAAGGGGCTATATAA
	R: CGTAGCTGTCTTTTTGTCCCATT
N-cadherin	F: GACAATGCCCCTCAAGTGTT
	R: CCATTAAGCCGAGTGATGGT
Vimentin	F: GAGAACTTTGCCGTTGAAGC
	R: TCCAGCAGCTTCCTGTAGGT
FN	F: ACCAACCTACGGATGACTCG
	R: GCTCATCATCTGGCCATTTT
Snail	F: ACCCCACATCCTTCTCACTG
	R: TACAAAAACCCACGCAGACA
GAPDH	F: AGAAGGCTGGGGCTCATTTG
	R: AGGGGCCATCCACAGTCTTC

F, forward; R, reverse; ZO-1, zonula occludens-1; α-SMA, α-smooth muscle actin; FN, fibronectin.

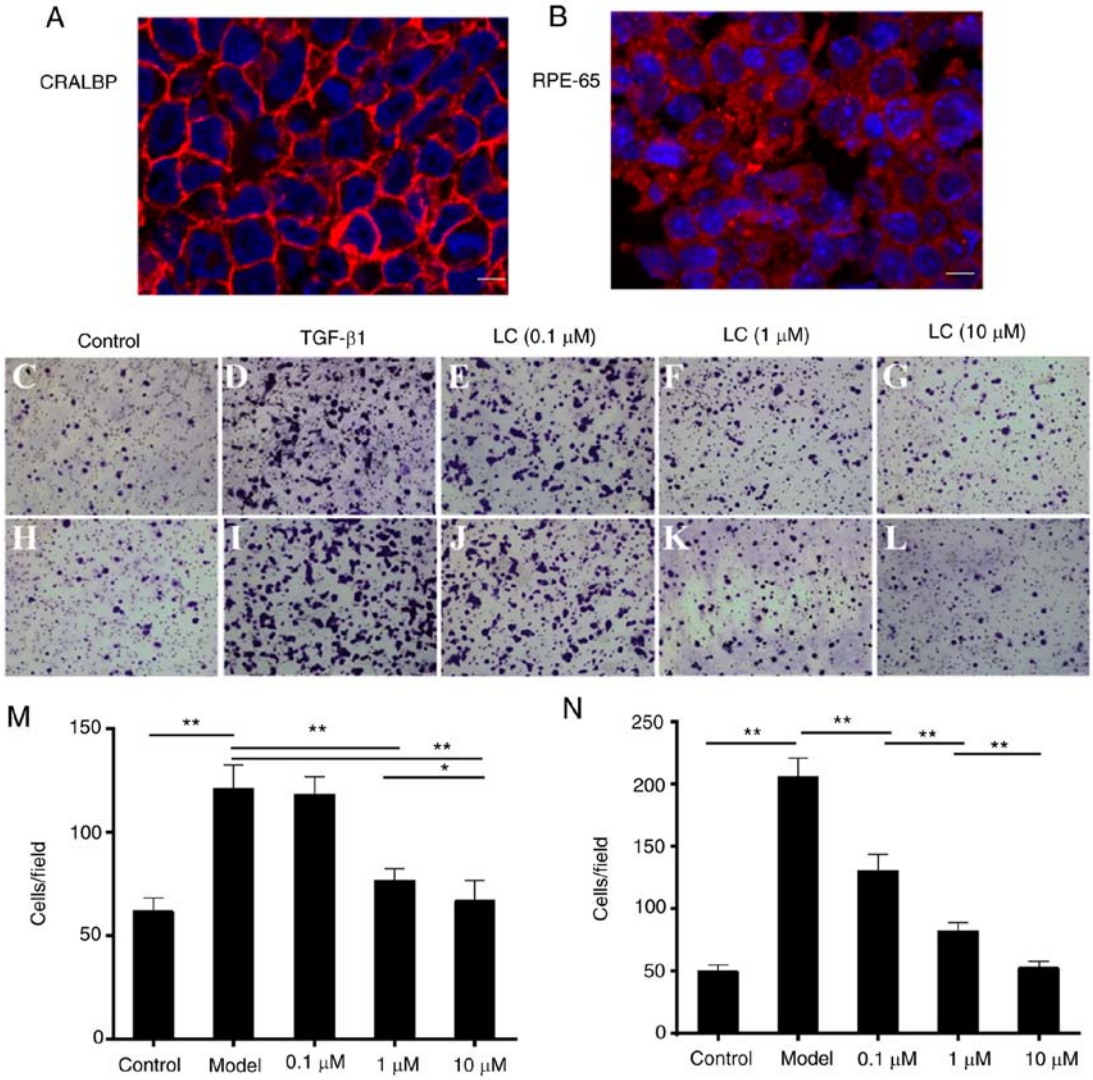

Figure 1. LC attenuates the migration of ARPE-19 cells. Immunofluorescence analysis of (A) CRALBP and (B) RPE-65 of ARPE-19 cells. Magnification, x630; scale bar, 10 μm. (C-L) Transwell analysis of ARPE-19 cells treated with TGF-β1 and LC. ARPE-19 cells were treated with 10 ng/ml TGF-β1 with or without 0.1, 1 and 10 μM LC for (C-G) 24 and (H-L) 48 h, and then a Transwell migration assay was performed. Number of migratory cells after (M) 24 and (N) 48 h of treatment with LC. *P<0.05, **P<0.01. LC, L-carnitine; CRALBP, cellular retinaldehyde-binding protein; RPE-65, retinoid isomerohydrolase.

and were analyzed using SPSS 20.0 software (IBM Corp.). An unpaired Student's t-test was used for comparisons between two groups. One-way ANOVA followed by Tukey's post hoc test were used to compare differences between multiple groups. P<0.05 was considered to indicate a statistically significant difference.

Results

Concentration-dependent effects of LC on the migratory activity of ARPE-19 cells. ARPE-19 cells used in this study showed expression of CRALBP (Fig. 1A) and RPE-65 (Fig. 1B). The number of migrated cells was significantly lower with increasing concentrations of LC (Fig. 1C-N). After 24 h of treatment, the number of migrated cells was lowered by co-culture with the LC concentrations of 1 μM (Fig. 1F and M) and 10 μM (Fig. 1G and M). Furthermore, the number of migrated cells was reduced significantly at an LC concentration of 0.1 μM (Fig. 1J and N) after 48 h of treatment.

LC prevents TGF-β1-induced EMT in RPE cells. To investigate whether LC prevented TGF-β1-induced EMT in RPE cells, the expression levels of epithelial markers (E-cadherin and ZO-1) and mesenchymal markers (α-SMA, vimentin, FN and N-cadherin) were determined. As shown in Fig. 2A and B, 10 ng/ml TGF-β1 led to an increase in the expression levels of α-SMA and FN, and decreased the expression levels of E-cadherin and ZO-1. These effects were reversed by treatment with 10 μM LC in ARPE-19 cells. There were no significant differences between 1 and 10 μM LC on E-cadherin, ZO-1 and FN expression. However, the expression of α-SMA and Snail in the 10 μM LC group was significantly lower than the 1 μM LC group. Furthermore, following treatment with increasing concentrations of LC, ARPE-19 cells displayed higher expression of E-cadherin and ZO-1 than in cells of the control group. Expression of α-SMA, FN, vimentin, N-cadherin and transcription factor Snail were notably lower at the mRNA (Fig. 2C) and protein (Fig. 2D) levels. The human primary RPE cells are presented in Fig. 2E. The same trend was observed in human RPE cells, as shown in Fig. 2F and G, TGF-β1 significantly promoted the expression of

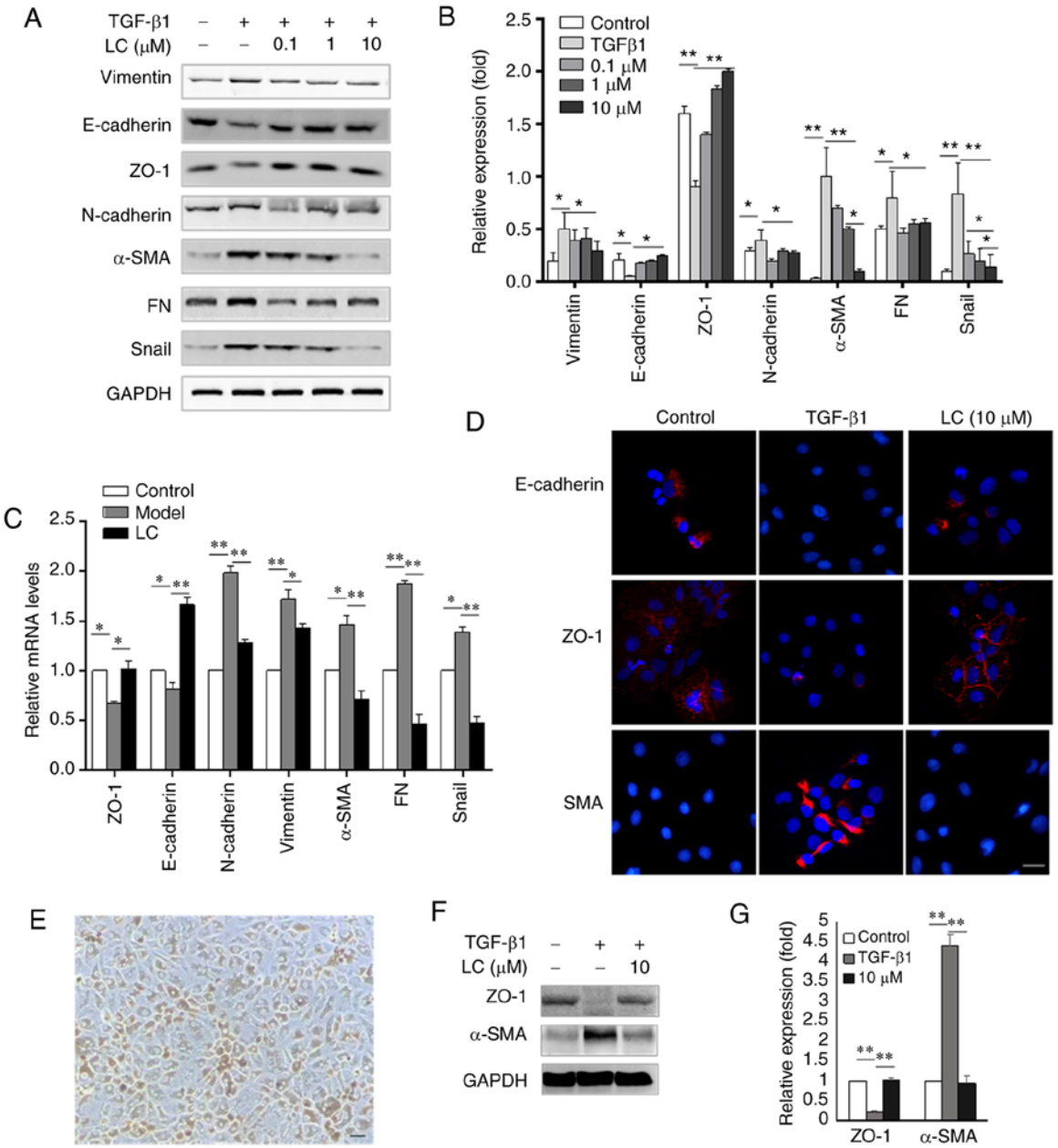

Figure 2. LC attenuates TGF-β1-induced epithelial-mesenchymal transition in ARPE-19 cells and human primary RPE cells. ARPE-19 cells were treated with 10 ng/ml TGF-β1 with or without LC (0.1, 1 and 10 μM) for 48 h. Human RPE cells were treated with 10 ng/ml TGF-β1 with or without 10 μM LC for 48 h. (A) Protein levels of vimentin, E-cadherin, ZO-1, N-cadherin, α-SMA, FN and Snail were detected using the corresponding antibodies in ARPE-19 cells. (B) Semi-quantification of protein levels from three independent experiments. (C) The mRNA expression levels of ZO-1, E-cadherin, N-cadherin, vimentin, α-SMA, FN and Snail were evaluated via reverse transcription-quantitative PCR. (D) The slides were observed by phase contrast microscopy. Magnification, x400. Nuclei were stained with DAPI. (E) The cultured human primary RPE cells. Magnification, x400. (F) Protein levels of ZO-1 and α-SMA were detected using the corresponding antibodies in human primary RPE cells. (G) Semi-quantification of protein levels from three independent experiments. *P<0.05, **P<0.01. LC, L-carnitine; ZO-1, zonula occludens-1; α-SMA, α-smooth muscle actin; FN, fibronectin; RPE, retinal pigment epithelial.

α-SMA and reduced the expression of ZO-1, and this process could be reversed by LC (Fig. 2F and G).

LC inhibits TGF-β1-induced EMT by suppressing MAPK pathways. The effects of LC on TGF-β1 signaling pathways in ARPE-19 cells (Fig. 3A-C) and human primary RPE cells (Fig. 3D-F) were investigated. LC had no effect on the canonical Smad2/3 signaling pathway. p-Erk1/2 and p-JNK expression levels were significantly lower in 10 μM LC-treated cells than in the TGF-β1 group, whereas the total Erk1/2, JNK, p38 and p-p38 expression were not affected.

PPARγ and NF-κB are involved in the inhibitory effect of LC on the EMT of RPE cells. To the best of our knowledge, LC inhibits the EMT of renal tubular epithelial cells via a PPARγ-dependent mechanism (13). NF-κB also plays a vital role in the EMT of RPE cells (24). Therefore, the present study next investigated the role of PPARγ and NF-κB in the inhibitory effect of LC on the EMT of RPE cells. As presented in Fig. 4A-C, treatment of ARPE-19 cells with TGF-β1 resulted in a marked increase in the expression of p-p105, p-p65 and p-IκB. These effects, with the exception of p-p105, were suppressed by LC. PPARγ expression was lower in ARPE-19

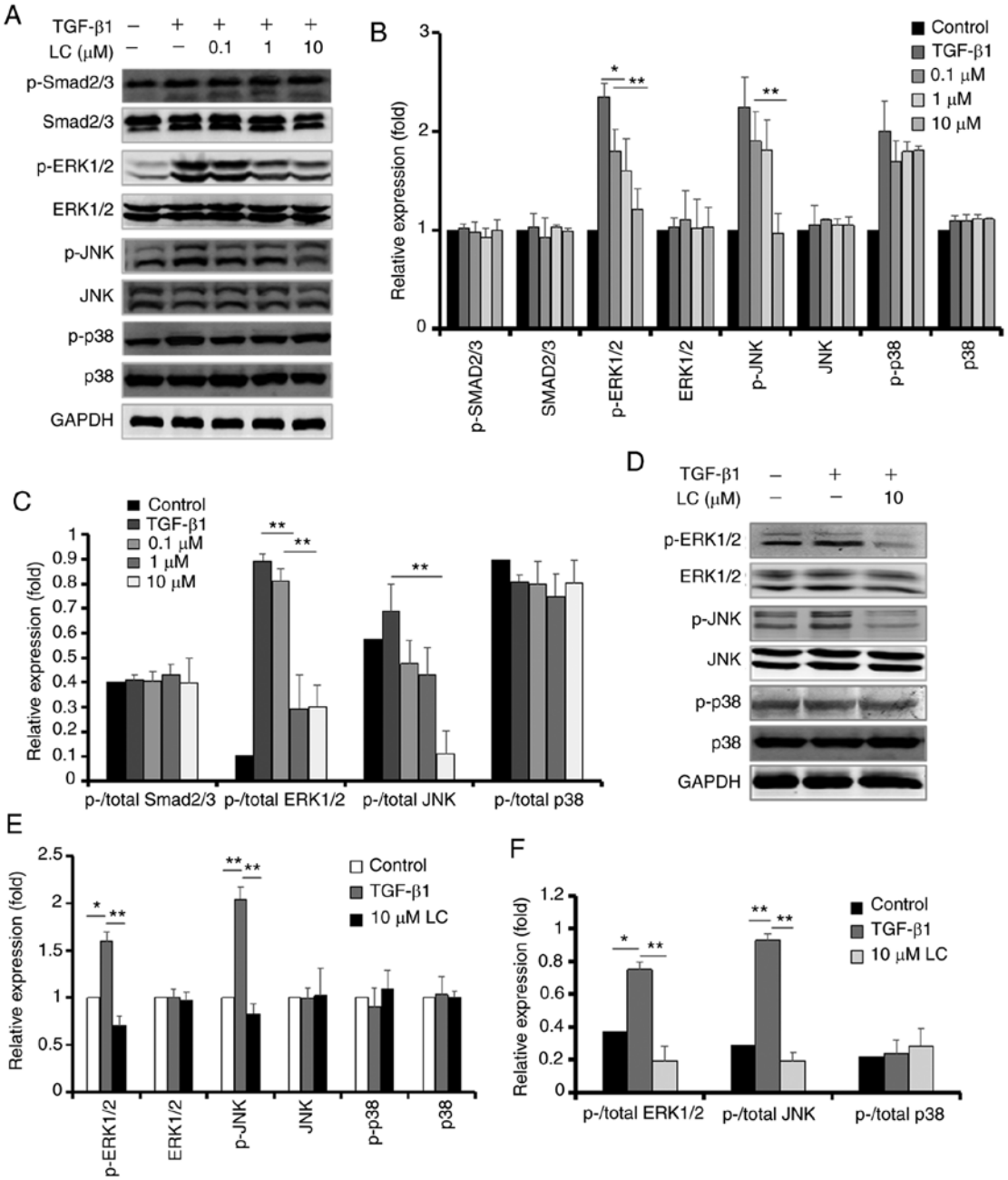

Figure 3. Protein levels of p-Smad2/3 and MAPK pathway-related markers in ARPE-19 cells and human primary RPE cells. (A) After ARPE-19 cells were treated with 10 ng/ml TGF-β1 with or without LC (0.1, 1 and 10 μM) for 48 h, p-Smad2/3, Smad2/3, ERK1/2, p-ERK1/2, JNK, p-JNK, p38 and p-p38 were detected using the corresponding antibody. (B) Semi-quantification of protein levels from three independent experiments. (C) The ratio of p-/total Smad2/3 protein, p-/total ERK1/2 protein, p-/total JNK protein and p-/total p38 protein. (D) After human RPE cells were treated with 10 ng/ml TGF-β1 with or without 10 μM LC for 48 h, p-ERK1/2, ERK1/2, p-JNK, JNK, p-p38 and p38 were detected. (E) Semi-quantification of protein levels from three independent experiments. (F) The ratio of p-/total ERK1/2 protein, p-/total JNK protein and p-/total p38 protein in the graph. *P<0.05, **P<0.01. LC, L-carnitine; p-, phosphorylated; RPE, retinal pigment epithelial.

cells after treatment with TGF-β1, which was reversed by LC. In human primary RPE cells, TGF-β1 upregulated the expression of p-p65 and downregulated the expression of PPARγ, and LC also inhibited these changes (Fig. 4D-F).

Inhibitory effect of LC on EMT is blocked by a PPAR-γ inhibitor. To further explore whether PPAR-γ was the critical factor of LC on EMT of RPE cells, a PPAR-γ inhibitor (GW9662) was used. ARPE-19 cells showed the typical mesenchymal markers after treatment with TGF-β1 (Fig. 2A and D), as shown by the upregulation of Vimentin, N-Cadherin, α-SMA and FN expression. LC attenuated the EMT effect of TGF-β1 on RPE cells. Inhibition of LC on EMT was blocked by GW9662 (Fig. 5A and B). A similar trend was detected in human primary RPE cells (Fig. 5C and D).

Relationships among the JNK signaling pathway, ERK signaling pathway, PPARγ and NF-κB on EMT of RPE cells. To investigate the underlying signaling pathways, inhibitors of JNK, ERK and PPARγ were used to explore their associations with each other. As shown in Fig. 6A-C, p-JNK and p-ERK protein expression were significantly lower after treatment with

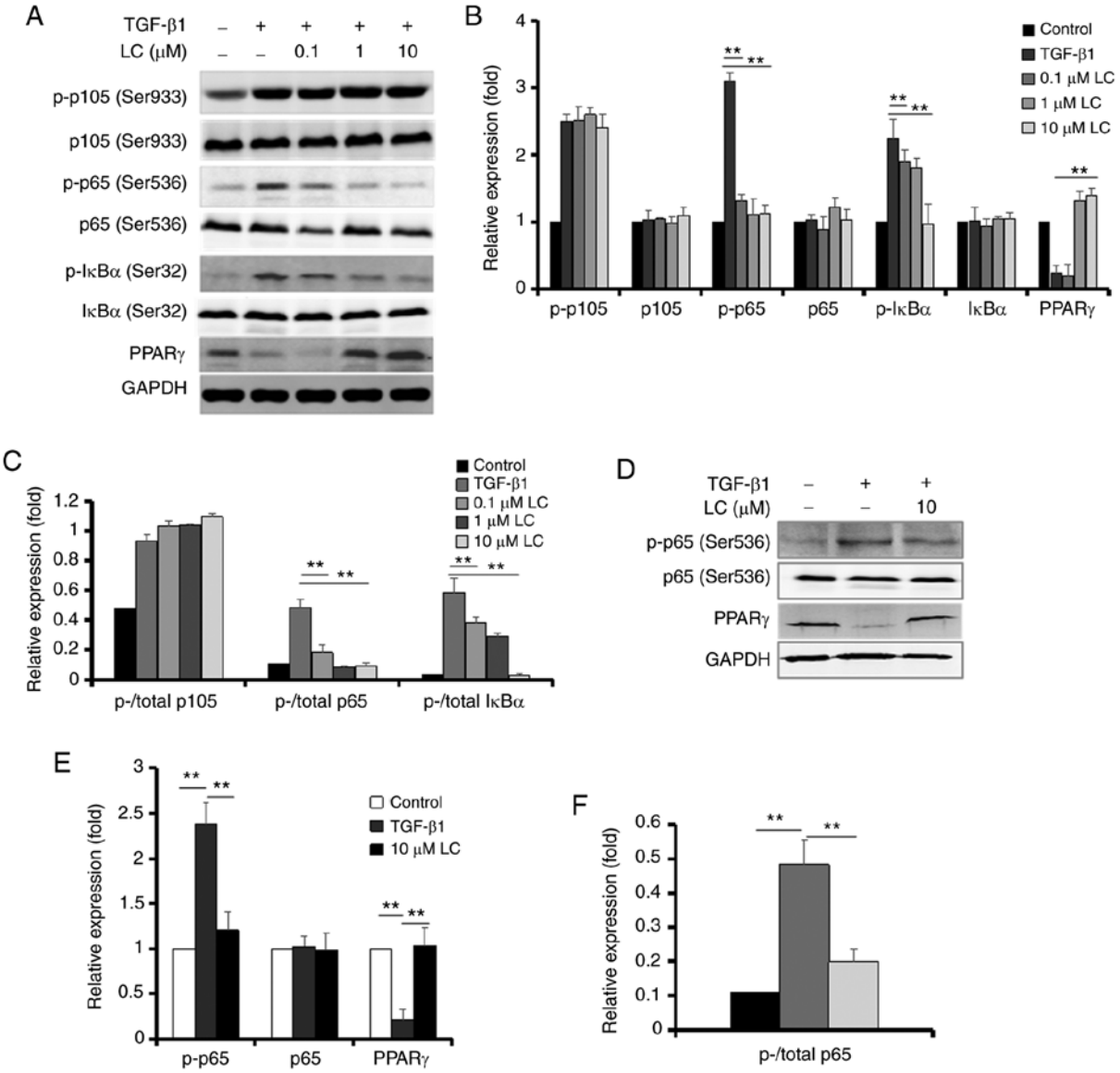

Figure 4. Protein levels of NF-κB and PPARγ in ARPE-19 cells and human primary RPE cells treated with TGF-β1 and LC. (A) After ARPE-19 cells were treated with 10 ng/ml TGF-β1 with or without LC (0.1, 1 and 10 μM) for 48 h, p-p105, p105, p-p65, p65, p-IκBα, IκBα and PPARγ were detected using the corresponding antibody. (B) Semi-quantification of protein levels from three independent experiments. (C) The ratio of p-/total p105 protein, p-/total p65 protein and p-/total IκB protein in the graph. (D) After human RPE cells were treated with 10 ng/ml TGF-β1 with or without 10 μM LC for 48 h, p-p65, p65 and PPARγ were detected. (E) Semi-quantification of protein levels from three independent experiments. (F) The ratio of p-/total p65 protein in the graph. **P<0.01. NF-κB, nuclear factor-κB; PPARγ, peroxisome proliferator-activated receptor γ; LC, L-carnitine; p-, phosphorylated; RPE, retinal pigment epithelial.

JNK and ERK inhibitors (SP600125 and U0126, respectively), leading to the upregulation of PPAR-γ and downregulation of p-p65. Furthermore, GW9662 did not affect upregulation of p-JNK and p-ERK induced by TGF-β1, but it downregulated the expression of p-p65.

Discussion

EMT in RPE cells is proposed to be a vital trigger in PVR (3,4,10,11). A number of studies have demonstrated this effect in response to various cytokines, especially TGF-β1, in the process of PVR formation (3,4,10,11). In our previous study, LC reduced EMT in RPE cells. LC, a quaternary ammonium compound, is synthesized from methionine and lysine. It transports fatty acids from the cytosol to the mitochondria for processing in lipid catabolism (25). Recently, LC was found to play vital roles in oxidative (26) and fibrotic diseases (21). To the best of our knowledge, the present study was the first to show that LC inhibited TGF-β1-induced EMT in RPE cells. Moreover, it was also found that LC prevented TGF-β1-induced EMT via controlling the JNK and ERK1/2 pathways, not the classical Smad signaling pathway. Finally, it was demonstrated that PPARγ was a critical factor in the underlying mechanism of LC on EMT in RPE cells.

Recent reports have shown that LC is associated with various pathological conditions. Chou *et al* (13) found that L-carnitine reversed the EMT induction caused by perfluorooctanesulfonate in renal tubular epithelial cells and alleviated cell migration by activating PPARγ. LC was also reported to attenuate cardiac fibrosis caused by sunitinib in hypertensive rats, which was dependent on NF-κB (27). In another previous report, LC attenuated liver fibrosis via

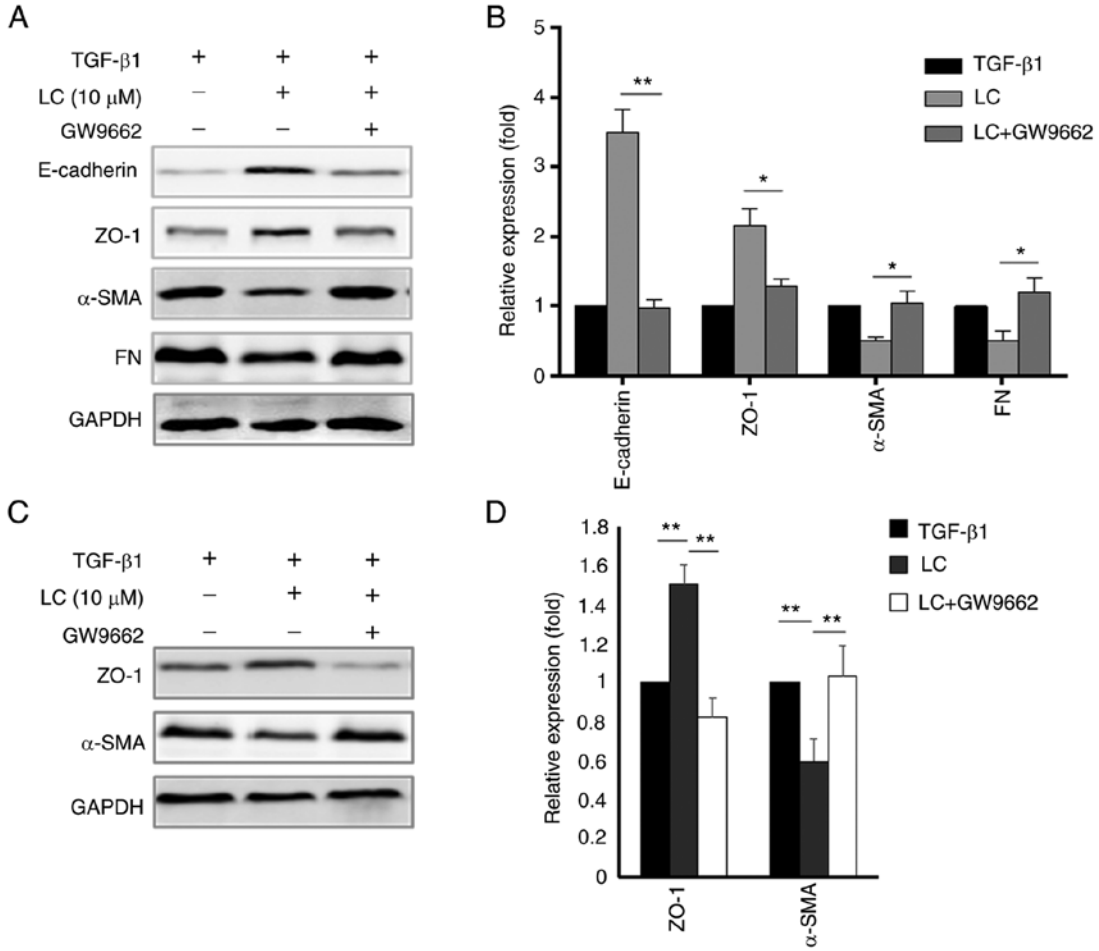

Figure 5. Effect of GW9662 on the epithelial-mesenchymal transition of RPE cells induced by TGF-β1. (A) After ARPE-19 cells were treated with 10 ng/ml TGF-β1 with LC (10 μM) and GW9662 for 48 h, E-cadherin, ZO-1, α-SMA and FN were detected using the corresponding antibody. (B) Semi-quantification of protein levels from three independent experiments. (C) After human primary RPE cells were treated with 10 ng/ml TGF-β1 with LC (10 μM) and GW9662 for 48 h, ZO-1 and α-SMA were detected. (D) Semi-quantification of protein levels from three independent experiments. *P<0.05, **P<0.01. LC, L-carnitine; ZO-1, zonula occludens-1; α-SMA, α-smooth muscle actin; FN, fibronectin; RPE, retinal pigment epithelial.

upregulation of the mitochondrial pathway (25). Nevertheless, to our knowledge, there has been no report concerning the role of LC in the EMT of RPE cells. To test the hypothesis that LC abrogates TGF-β1-induced EMT in RPE cells, ARPE-19 cells and human primary RPE cells were cultured with TGF-β1 and LC in the present study. It was found that the expression levels of epithelial markers were significantly increased, whereas mesenchymal markers and mobility of RPE cells were significantly decreased with increasing concentrations of LC. Taken together, the data suggested that 10 μM LC could be useful for abrogating EMT in RPE cells.

The downstream pathways of TGF-β1 include not only the canonical Smad2/3 signaling pathway, but also the non-canonical p38/MAPK, JNK and ERK1/2 pathways (28,29). Although the Smad2/3 signaling pathway plays an important role in TGF-β1-induced RPE cell EMT, several lines of evidence have shown that MAPK pathways integrate with the Smad2/3 signaling pathway to mediate EMT (28,30). In RPE cells, the present study also demonstrated that the non-canonical JNK and ERK1/2 pathways were activated by TGF-β1, as well as the canonical Smad2/3 signaling pathway. Finally, LC was found to attenuate TGF-β1-induced phosphorylation of JNK and ERK1/2, but not Smad2/3 directly.

Several studies have reported that LC alleviates EMT and tissue fibrosis via a PPARγ-dependent mechanism in the kidney and heart (13,21,27). Of note, another previous study demonstrated that GW9662 was a poor inhibitor of fibroblast-to-myofibroblast differentiation (31). Therefore, in order to explore whether this inhibition of TGF-β1-induced EMT on RPE cells was PPARγ-dependent, the PPARγ antagonist GW9662 was used in combination with LC. It was found that, without PPARγ, LC did not inhibit RPE cell EMT. That is to say, the inhibitory effect of LC on RPE cells was PPARγ-dependent, similar to results from Zambrano *et al* (21) and Blanca *et al* (27).

NF-κB-Snail signaling is hypothesized to play a vital role in EMT, tumor cell invasion and metastasis. It regulates the EMT process via decreasing expression of various epithelial markers (32) and by increasing expression of mesenchymal markers (33). In fact, we previously showed that Snail activation was important in the EMT of RPE cells induced by TGF-β1 (34,35). In the present study, it was demonstrated that LC significantly decreased NF-κB and Snail expression at the protein level. These results may partly explain the underlying mechanism of the inhibitory effect of LC on the EMT process.

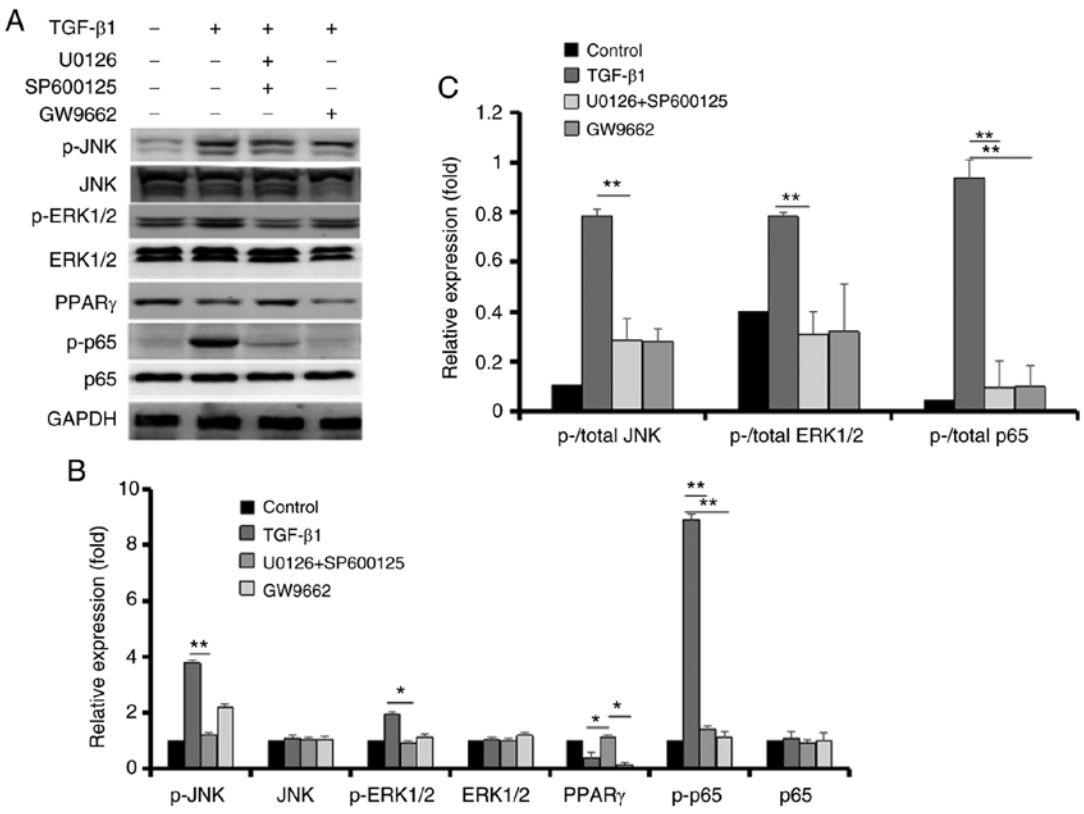

Figure 6. Effects of U0126, SP600125 and GW9662 on the expression of p-JNK, JNK, p-ERK1/2, ERK1/2, PPARγ, p-p65 and p65 in retinal pigment epithelial cells. (A) After ARPE-19 cells were treated with 10 ng/ml TGF-β1 with or without U0126, SP600125 and GW9662 for 48 h, p-JNK, JNK, p-ERK1/2, ERK1/2, PPARγ, p-p65 and p65 were detected using the corresponding antibody. (B) Semi-quantification of protein levels from three independent experiments. (C) The ratio of p-/total JNK protein, p-/total ERK1/2 protein and p-/total p65 protein in the graph. *P<0.05, **P<0.01. LC, L-carnitine; p-, phosphorylated; PPARγ, peroxisome proliferator-activated receptor γ.

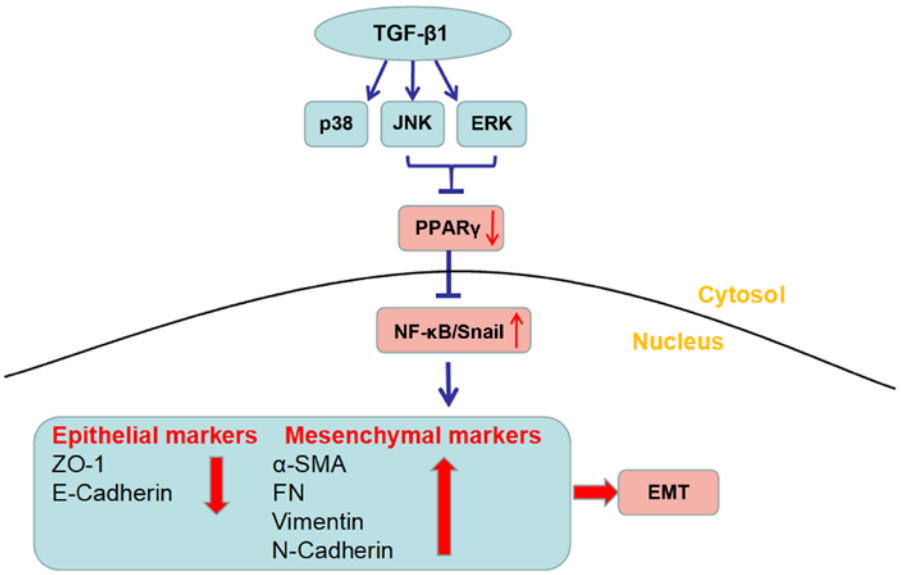

Figure 7. Proposed mechanism of the inhibitory effect of L-carnitine on the EMT of retinal pigment epithelial cells induced by TGF-β1. EMT, epithelial-mesenchymal transition; ZO-1, zonula occludens-1; α-SMA, α-smooth muscle actin; FN, fibronectin; NF-κB, nuclear factor-κB; PPARγ, peroxisome proliferator-activated receptor γ.

In summary, the current study provided evidence for the first time that LC inhibited TGF-β1-induced EMT in RPE cells. The mechanism underlying this process was found to be inactivation of non-Smad pathways, including ERK1/2 and JNK pathways. Moreover, the inhibitory effect of LC on RPE cells was revealed to be PPARγ-dependent. Fig. 7 presents an outline of the proposed underlying mechanism. The present study supports the notion that LC has inhibitory effects on EMT in RPE cells. However, there are limitations of the present study as most assays in this study were performed

using ARPE-19 cells due to the limited number of primary human RPE cells. Also, no control cell line was used in this study. Based on these results, we are also exploring further effects on the primary human RPE cells and the effects of LC injected into PVR model rat eyes. The *in vivo* data will be presented in another future article.

To conclude, this study suggested that LC attenuated EMT via inhibition of the Erk1/2 and JNK pathways, which was dependent on PPAR-γ expression. LC may have potential value in the prevention and treatment of PVR.

Acknowledgements

Not applicable.

Funding

This study was funded by a grant from the National Natural Science Foundation of China (grant no. 81500727) and the Fundamental Research Funds for the Central Universities (grant no. 22120180053).

Availability of data and materials

The datasets used and/or analyzed during the current study are available from the corresponding author on reasonable request.

Authors' contributions

ML and FW designed this study. ML, HL and SY performed the experiments. XL and CZ analyzed the data. ML and HL drafted this article. CZ and FW revised the article. ML, HL and SY confirm the authenticity of all the raw data. All authors read and approved the final manuscript.

Ethics approval and consent to participate

This study was approved by the Ethics Committee of Shanghai Tenth People's Hospital (Shanghai, China) and was in compliance with the Declaration of Helsinki. Donors' eyes were obtained from the Eye Bank of Shanghai Tenth People's Hospital.

Patient consent for publication

Not applicable.

Competing interests

The authors declare that they have no competing interests.

References

1. Gartry DS, Chignell AH, Franks WA and Wong D: Pars plana vitrectomy for the treatment of rhegmatogenous retinal detachment uncomplicated by advanced proliferative vitreoretinopathy. Br J Ophthalmol 77: 199-203, 1993.
2. Leiderman YI and Miller JW: Proliferative vitreoretinopathy: Pathobiology and therapeutic targets. Semin Ophthalmol 24: 62-69, 2009.
3. Pastor JC, de la Rúa ER and Martín F: Proliferative vitreoretinopathy: Risk factors and pathobiology. Prog Retin Eye Res 21: 127-144, 2002.
4. Yu J, Liu F, Cui SJ, Liu Y, Song ZY, Cao H, Chen FE, Wang WJ, Sun T and Wang F: Vitreous proteomic analysis of proliferative vitreoretinopathy. Proteomics 8: 3667-3678, 2008.
5. Kurimoto R, Iwasawa S, Ebata T, Ishiwata T, Sekine I, Tada Y, Tatsumi K, Koide S, Iwama A and Takiguchi Y: Drug resistance originating from a TGF-β/FGF-2-driven epithelial-to-mesenchymal transition and its reversion in human lung adenocarcinoma cell lines harboring an EGFR mutation. Int J Oncol 48: 1825-1836, 2016.
6. Kim J, Kong J, Chang H, Kim H and Kim A: EGF induces epithelial-mesenchymal transition through phospho-Smad2/3-Snail signaling pathway in breast cancer cells. Oncotarget 7: 85021-85032, 2016.
7. Garweg JG, Tappeiner C and Halberstadt M: Pathophysiology of proliferative vitreoretinopathy in retinal detachment. Surv Ophthalmol 58: 321-329, 2013.
8. Lamouille S and Derynck R: Cell size and invasion in TGF-beta-induced epithelial to mesenchymal transition is regulated by activation of the mTOR pathway. J Cell Biol 178: 437-451, 2007.
9. Charteris DG: Proliferative vitreoretinopathy: Pathobiology, surgical management, and adjunctive treatment. Br J Ophthalmol 79: 953-960, 1995.
10. Li M, Li H, Liu X, Xu D and Wang F: MicroRNA-29b regulates TGF-β1-mediated epithelial-mesenchymal transition of retinal pigment epithelial cells by targeting AKT2. Exp Cell Res 345: 115-124, 2016.
11. Yao H, Li H, Yang S, Li M, Zhao C, Zhang J, Xu G and Wang F: Inhibitory effect of bone morphogenetic protein 4 in retinal pigment epithelial-mesenchymal transition. Sci Rep 2: 32182, 2016.
12. Martin H: Role of PPAR-gamma in inflammation. Prospects for therapeutic intervention by food components. Mutat Res 690: 57-63, 2010.
13. Chou HC, Wen LL, Chang CC, Lin CY, Jin L and Juan SH: From the Cover: l-Carnitine via PPARγ- and Sirt1-dependent mechanisms attenuates epithelial-mesenchymal transition and renal fibrosis caused by perfluorooctanesulfonate. Toxicol Sci 160: 217-229, 2017.
14. Ferguson HE, Kulkarni A, Lehmann GM, Garcia-Bates TM, Thatcher TH, Huxlin KR, Phipps RP and Sime PJ: Electrophilic peroxisome proliferator-activated receptor-gamma ligands have potent antifibrotic effects in human lung fibroblasts. Am J Respir Cell Mol Biol 41: 722-730, 2009.
15. Kao HF, Chang-Chien PW, Chang WT, Yeh TM and Wang JY: Propolis inhibits TGF-β1-induced epithelial-mesenchymal transition in human alveolar epithelial cells via PPARγ activation. Int Immunopharmacol 15: 565-574, 2013.
16. Fang IM, Yang CH and Yang CM: Docosahexaenoic acid reduces linoleic acid induced monocyte chemoattractant protein-1 expression via PPARγ and nuclear factor-κB pathway in retinal pigment epithelial cells. Mol Nutr Food Res 58: 2053-2065, 2014.
17. Willermain F, Dulku S, Gonzalez NS, Blero D, Driessens G, De Graef C, Caspers L and Bruyns C: 15-Deoxy-12,14-prostaglandin J2 inhibits interferon gamma induced MHC class II but not class I expression on ARPE cells through a PPAR gamma independent mechanism. Prostaglandins Other Lipid Mediat 80: 136-143, 2006.
18. Rolim LC, da Silva EM, Flumignan RL, Abreu MM and Dib SA: Acetyl-L-carnitine for the treatment of diabetic peripheral neuropathy. Cochrane Database Syst Rev 6: CD011265, 2019.
19. Li M, Li H, Jiang P, Liu X, Xu D and Wang F: Investigating the pathological processes of rhegmatogenous retinal detachment and proliferative vitreoretinopathy with metabolomics analysis. Mol Biosyst 10: 1055-1062, 2014.
20. Baci D, Bruno A, Bassani B, Tramacere M, Mortara L, Albini A and Noonan DM: Acetyl-L-carnitine is an anti-angiogenic agent targeting the VEGFR2 and CXCR4 pathways. Cancer Lett 429: 100-116, 2018.
21. Zambrano S, Blanca AJ, Ruiz-Armenta MV, Miguel-Carrasco JL, Arévalo M, Mate A and Vázquez CM: L-carnitine attenuates the development of kidney fibrosis in hypertensive rats by upregulating PPAR-γ. Am J Hypertens 27: 460-470, 2014.
22. Parapuram SK, Ganti R, Hunt RC and Hunt DM: Vitreous induces components of the prostaglandin E2 pathwayaglandin E2 pathway in human retinal pigment epithelial cells. Invest Ophthalmol Vis Sci 44: 1767-1774, 2003.
23. Livak KJ and Schmittgen TD: Analysis of relative gene expression data using real-time quantitative PCR and the 2(-Delta Delta C(T)) method. Methods 25: 402-408, 2001.

24. Chen Z, Mei Y, Lei H, Tian R, Ni N, Han F, Gan S and Sun S: LYTAK1, a TAK1 inhibitor, suppresses proliferation and epithelial-mesenchymal transition in retinal pigment epithelium cells. Mol Med Rep 14: 145-150, 2016.
25. Ishikawa H, Takaki A, Tsuzaki R, Yasunaka T, Koike K, Shimomura Y, Seki H, Matsushita H, Miyake Y, Ikeda F, *et al*: L-carnitine prevents progression of non-alcoholic steatohepatitis in a mouse model with upregulation of mitochondrial pathway. PLoS One 9: e100627, 2014.
26. Ferreira GC and McKenna MC: L-Carnitine and Acetyl-L-carnitine roles and neuroprotection in developing brain. Neurochem Res 42: 1661-1675, 2017.
27. Blanca AJ, Ruiz-Armenta MV, Zambrano S, Miguel-Carrasco JL, Arias JL, Arévalo M, Mate A, Aramburu O and Vázquez CM: Inflammatory and fibrotic processes are involved in the cardiotoxic effect of sunitinib: Protective role of L-carnitine. Toxicol Lett 241: 9-18, 2016.
28. Ling G, Ji Q, Ye W, Ma D and Wang Y: Epithelial-mesenchymal transition regulated by p38/MAPK signaling pathways participates in vasculogenic mimicry formation in SHG44 cells transfected with TGF-β cDNA loaded lentivirus *in vitro* and *in vivo*. Int J Oncol 49: 2387-2398, 2016.
29. Park JH, Yoon J, Lee KY and Park B: Effects of geniposide on hepatocytes undergoing epithelial-mesenchymal transition in hepatic fibrosis by targeting TGFβ/Smad and ERK-MAPK signaling pathways. Biochimie 113: 26-34, 2015.
30. Zhou X, Kuang X, Long C, Liu W, Tang Y, Liu L, Liu H, He J, Huang Z, Fan Y, *et al*: Curcumin inhibits proliferation and epithelial-mesenchymal transition of retinal pigment epithelial cells via multiple pathways. Curr Mol Med 17: 312-319, 2017.
31. Zhou BY, Buckley ST, Patel V, Liu YX, Luo J, Krishnaveni MS, Ivan M, DeMaio L, Kim KJ, Ehrhardt C, *et al*: Troglitazone attenuates TGF-β1-induced EMT in alveolar epithelial cells via a PPARγ-independent mechanism. PLoS One 7: e38827, 2012.
32. Han D, Wu G, Chang C, Zhu F, Xiao Y, Li Q, Zhang T and Zhang L: Disulfiram inhibits TGF-β-induced epithelial-mesenchymal transition and stem-like features in breast cancer via ERK/NF-κB/Snail pathway. Oncotarget 6: 40907-40919, 2015.
33. Cho IH, Jang EH, Hong D, Jung B, Park MJ and Kim JH: Suppression of LPS-induced epithelial-mesenchymal transition by aqueous extracts of *Prunella vulgaris* through inhibition of the NF-κB/Snail signaling pathway and regulation of EMT-related protein expression. Oncol Rep 34: 2445-2450, 2015.
34. Li H, Li M, Xu D, Zhao C, Liu G and Wang F: Overexpression of Snail in retinal pigment epithelial triggered epithelial-mesenchymal transition. Biochem Biophys Res Commun 446: 347-351, 2014.
35. Li H, Chang HM, Shi Z and Leung PCK: SNAIL mediates TGF-β1-induced downregulation of pentraxin 3 expression in human granulosa cells. Endocrinology 159: 1644-1657, 2018.